Research Article

Cancer Immunology Research

Preserved Activity of CD20-Specific Chimeric Antigen Receptor–Expressing T Cells in the Presence of Rituximab

Gregory A. Rufener[1], Oliver W. Press[1,2], Philip Olsen[1], Sang Yun Lee[1], Michael C. Jensen[1,3], Ajay K. Gopal[1,2], Barbara Pender[1], Lihua E. Budde[4], Jeffrey K. Rossow[1], Damian J. Green[1,2], David G. Maloney[1,2], Stanley R. Riddell[1,2], and Brian G. Till[1,2]

Abstract

CD20 is an attractive immunotherapy target for B-cell non-Hodgkin lymphomas, and adoptive transfer of T cells genetically modified to express a chimeric antigen receptor (CAR) targeting CD20 is a promising strategy. A theoretical limitation is that residual serum rituximab might block CAR binding to CD20 and thereby impede T cell–mediated anti-lymphoma responses. The activity of CD20 CAR-modified T cells in the presence of various concentrations of rituximab was tested *in vitro* and *in vivo*. CAR-binding sites on $CD20^+$ tumor cells were blocked by rituximab in a dose-dependent fashion, although at 37°C blockade was incomplete at concentrations up to 200 μg/mL. T cells with CD20 CARs also exhibited modest dose-dependent reductions in cytokine secretion and cytotoxicity, but not proliferation, against lymphoma cell lines. At rituximab concentrations of 100 μg/mL, CAR T cells retained ≥50% of baseline activity against targets with high CD20 expression, but were more strongly inhibited when target cells expressed low CD20. In a murine xenograft model using a rituximab-refractory lymphoma cell line, rituximab did not impair CAR T-cell activity, and tumors were eradicated in >85% of mice. Clinical residual rituximab serum concentrations were measured in 103 lymphoma patients after rituximab therapy, with the median level found to be only 38 μg/mL (interquartile range, 19–72 μg/mL). Thus, despite modest functional impairment *in vitro*, the *in vivo* activity of CD20-targeted CAR T cells remains intact at clinically relevant levels of rituximab, making use of these T cells clinically feasible.

Cancer Immunol Res; 4(6); 509–19. ©2016 AACR.

See related Spotlight by Sadelain, p. 473.

Introduction

Adoptive transfer of genetically modified T cells has emerged as a potent therapy for lymphoid malignancies. The most widely used strategy has been infusion of patient-derived T cells expressing chimeric antigen receptors (CAR) that target tumor-associated antigens. This approach has numerous theoretical advantages, including the ability to target T cells to any cell-surface antigen, circumvent loss of major histocompatibility complex as a tumor escape mechanism, and use a single vector construct to treat any patient, regardless of human leukocyte antigen haplotype. CAR clinical trials for B-cell non-Hodgkin lymphoma (NHL) have, to date, targeted CD19, CD20, or CD22—antigens that are expressed both on malignant lymphoid cells and on normal B cells (1–10). Most investigators target CD19 because it is expressed from earlier stages of B-cell differentiation than CD20 or CD22. CAR T cells targeting CD19 can therefore be used to treat a slightly wider range of B-cell malignancies, including acute lymphoblastic leukemia, which arises at the pro-B or pre-B cell stage of differentiation.

CD20 remains an appealing antigen, however, having an extensive clinical record as a successful immunotherapy target for monoclonal antibodies (mAb) like rituximab (11–14). In contrast with CD19, which is readily internalized upon antibody (Ab) binding (15), CD20 is much more slowly endocytosed (16, 17). This stability could theoretically have a positive impact on the quality of the immunologic synapse, resulting in more robust CAR triggering and T-cell activation. Loss of CD19 expression on tumor cells is an escape mechanism in patients treated with CD19-targeted T cells (18). Although CD20 loss has also been described following CD20 mAb therapy, CD20-specific CAR T cells provide an alternative target that would allow sequential therapy, or could be used in concert with CD19 CAR T cells to target multiple antigens simultaneously, reducing the risk of immune escape by antigen loss.

One potential limitation of CD20 as a target antigen for CARs is that patients with relapsed or refractory lymphoma who are likely to be candidates for CAR T-cell therapy trials will often have been treated recently with rituximab-containing regimens. Because Abs can persist in the serum for months, residual rituximab could theoretically block the binding of CARs to CD20 and prevent or weaken T-cell activation, potentially rendering the therapy ineffective. In our previous CD20 CAR T-cell trials (9, 10), eligibility criteria excluded patients recently treated with rituximab. However, this approach significantly affects accrual and would

[1]Clinical Research Division, Fred Hutchinson Cancer Research Center, Seattle, Washington. [2]Division of Medical Oncology, University of Washington School of Medicine, Seattle, Washington. [3]Seattle Children's Research Institute, Seattle, Washington. [4]City of Hope Medical Center, Duarte, California.

Corresponding Author: Brian G. Till, Fred Hutchinson Cancer Research Center, 1100 Fairview Avenue North, D3-100, Seattle, WA 98109. Phone: 206-667-7269; Fax: 206-667-1874; E-mail: tillb@fhcrc.org

doi: 10.1158/2326-6066.CIR-15-0276

ultimately limit the availability of this therapy for patients most in need of novel treatment options.

A few previous observations led us to question the assumption that residual CD20 mAbs would represent a major constraint for CD20-targeted CAR T cells. The activity of bispecific mAbs that bind both CD3 and CD20 and mediate cellular cytotoxicity by conjugating T cells to $CD20^+$ tumor cells is not blocked by rituximab concentrations up to 100 μg/mL (19), suggesting that only a few binding sites for CD20 need to be available for sufficient T-cell activation. Additionally, experiments using first-generation CD20 CARs demonstrated partial inhibition of cytokine secretion by rituximab, but T cells retained 40% to 60% of baseline function at concentrations of 20 to 50 μg/mL (20, 21). In a broader context, cytokine secretion and cytotoxicity of CAR T cells targeting carcinoembryonic antigen, Lewis-Y antigen, or CD30 are largely unimpaired in the presence of soluble cognate antigen concentrations of up to 10 μg/mL (22–25), although levels higher than this are potentially inhibitory (22).

In this study, we sought to test the effect of various rituximab concentrations on the activity of T cells expressing anti-CD20 CARs both *in vitro* and *in vivo* and found that CD20 CAR T-cell function was largely preserved in the presence of clinically relevant rituximab concentrations.

Materials and Methods

Cell lines

Raji, Daudi, and Ramos (Burkitt lymphoma), Rec-1 (mantle cell lymphoma), and K562 (CD20-negative erythroid leukemia) tumor cell lines were obtained from ATCC. Granta-519 (mantle cell lymphoma) was obtained from DSMZ, and FL-18 (transformed follicular lymphoma) was obtained from Dr. David Maloney [Fred Hutchinson Cancer Research Center (FHCRC), Seattle, Washington]. Cells were originally obtained between 2004 and 2010 and passaged for $\leq$1 month before experiments, and CD20 expression was authenticated by flow cytometry on all cell lines prior to experiments. Cell lines were cultured in RPMI-1640 with 25 mmol/L HEPES, 10% FBS, 1% penicillin/streptomycin, and 1% L-glutamine and incubated at 37°C in 5% CO_2. K562 cells were transduced with a lentiviral vector to express human CD80 and again with a retroviral vector to express CD20. Low, medium, and high CD20-expressing K562-CD80 cell lines were obtained by selection after limiting dilution cloning. Raji-ffLuc cells were produced by transduction of Raji cells with retrovirus encoding firefly luciferase-Thy1.1-Neo and selected with G418 as previously described (26). Rituximab-refractory Raji-ffLuc cells were generated with repeated, intermittent cycles of escalating rituximab concentrations as previously described (27).

Flow cytometry to assess CD20 blocking by rituximab

Ramos cell lines were incubated with rituximab concentrations ranging from 0 to 200 μg/mL at room temperature for 30 minutes. After CD20 blocking, CD20-PE mAb [clone L27 (Leu16), BD Biosciences] was added, and cells were incubated at either 4°C or 37°C for 30 minutes. Cells were washed with cold FACS buffer (0.5% fetal bovine serum and 2.5 mmol/L EDTA in PBS) and analyzed on a BD Canto 2 flow cytometer. Data were analyzed using FlowJo version 7.6.1 (TreeStar). In a separate experiment, FL-18 cells were blocked with varying concentrations of rituximab, washed once with FACS buffer, and then anti-CD20-FITC Ab (clone 1F5, produced in-house from a hybridoma; ref. 28) was added and incubated with blocked cells for 15 minutes at 4°C. Cells were then washed and analyzed as described above. Similar experiments were also conducted in which rituximab was replaced by ofatumumab, a fully human mAb to CD20 that binds to a different epitope.

Vector constructs

The CD20-specific Leu16-28-BB-z-tEGFR vector was constructed by amplifying the Leu16 single-chain variable-region fragment (scFv; refs. 29, 30) by PCR and cloning into NheI and RsrII sites of an epHIV7 lentiviral vector encoding IgG4-Fc, CD28, and 41BB domains, and the CD3ζ domain (ref. 31; GenBank accession # KX055828). The Leu16-28-z vector was generated by splice overlap PCR of the Leu16-28-BB-z-tEGFR vector to remove the 41BB domain and truncated EGFR (GenBank accession # KX055829). The lentiviral vector encoding the CD20-specific 1F5-28-BB-z CAR has been previously described (32), but was transferred to the HIV-1–based RRL.sin.cPPT.PGK.GFP.wpre self-inactivating third-generation lentiviral vector backbone (ref. 33; from Dr. Hans-Peter Kiem, FHCRC). The Fc spacer region of this construct was modified to abrogate binding to Fcγ receptors by substituting the IgG1 hinge linker with the IgG2 hinge linker and adding an N297Q mutation as previously described (34, 35), to create the 1F5-NQ-28-BB-z vector (GenBank accession # KX055830). To generate the 1.5.3-NQ-28-BB-z CAR construct, a novel scFv sequence was produced by synthesizing the V_L and V_H sequences from the 1.5.3 fully human anti-CD20 Ab (patent WO 2006/130458; ref. 36) using a codon optimization algorithm (GenScript), separated by a 15-amino-acid glycine-serine linker, preceded by the GM-CSF signal peptide. An overlapping fragment produced by splice overlap PCR was used to replace the scFv domain of the 1F5-NQ-28-BB-z vector, cloning it into AgeI/SacII restriction sites (GenBank accession # KX055831). The inducible caspase-9 suicide gene and downstream 2A sequence were removed from this construct by splice overlap PCR. The 1.5.3-NQ-28-z construct was generated by removing the 41BB domain from 1.5.3-NQ-28-BB-z by splice overlap PCR (GenBank accession # KX055832). All constructs were confirmed by Sanger sequencing. Lentivirus was produced using 293T cells transiently transfected with the described backbone vectors as well as the packaging vectors pCGHP-2, pCMV-Rev2, and pCMV-G, and supernatants containing packaged lentivirus were concentrated 100-fold by centrifugation.

T-cell isolation and transduction

Peripheral blood mononuclear cells (PBMC) were obtained either by apheresis from healthy donors consented under Institutional Review Board (IRB)–approved research protocols at the FHCRC or from used Pall leukocyte filters purchased from the Puget Sound Blood Center. PBMCs isolated by centrifugation with Ficoll–Paque density gradient medium underwent red blood cell lysis with ammonium–chloride–potassium (ACK) buffer and were cryopreserved in 10% DMSO and 90% FBS. For *in vitro* experiments, T cells were negatively selected from thawed PMBC by MACS using a Pan T-cell Isolation Kit II (Miltenyi Biotec). For cytotoxicity experiments, $CD8^+$ T cells were positively selected from healthy donor apheresis PBMC by MACS using CD8 mAb-coated beads (Miltenyi Biotec) prior to cryopreservation. For some experiments, central memory T cells (T_{CM}) were isolated from healthy donor apheresis PBMCs prior to cryopreservation by

negative selection using an AutoMACS device after incubation with CliniMACS anti-CD14 and anti-CD45RA beads (Miltenyi Biotec), followed by positive selection with CliniMACS anti-CD62L beads. T cells were stimulated with anti-CD3/anti-CD28 mAb-coated Human T-Expander Beads (Invitrogen) at a 3:1 bead: T-cell ratio. Activated T cells were spin-transduced (2,100 rpm for 60 minutes at 32°C) the next day with lentiviral vector encoding one of the CD20 CAR constructs (multiplicity of infection of 2–6) plus polybrene (4–8 μg/mL). Transduced T cells were cultured in media containing recombinant human interleukin 2 (rhIL2; 50 IU/mL) and rhIL15 (10 ng/mL; Miltenyi Biotec), incubated 5 days after stimulation before magnetic removal of anti-CD3/anti-CD28 beads, and analyzed by flow cytometry to confirm CAR expression. CAR^+ T cells were then used in functional assays.

For *in vivo* mouse experiments, T_{CM} were thawed, activated, and transduced the next day with concentrated 1.5.3-NQ-28-BB-z lentiviral supernatant. CD3/CD28 beads were removed on day 5, cells were expanded in rhIL2 (50 IU/mL), restimulated on day 10 with irradiated $CD20^+$ lymphoblastoid cells (LCL) at a 1:1 responder:stimulator ratio, and injected into mice 11 days after restimulation with LCLs.

Proliferation and cytokine secretion assays

Target cells were irradiated with 8,000 to 10,000 cGy and incubated for 30 minutes at room temperature with various rituximab (or ofatumumab, as indicated) concentrations. T cells (2×10^5 total cells) stained with 5 μmol/L carboxyfluorescein succinimidyl ester (CFSE) were then cocultured at 1:1 ratios with rituximab-blocked tumor target lines. Supernatant was collected 24 hours after plating and stored at −20°C until subsequent cytokine analysis by Luminex assay as previously described (10) to quantify IFNγ, IL2, and TNFα. After 4 to 5 days, cells were stained with anti-CD3-APC (BioLegend), and CFSE dilution of CD3-gated lymphocytes as a measure of proliferation was determined by flow cytometry. Cell size as another measure of activation was determined by flow cytometry using the geometric mean of the forward scatter (FSC-A) parameter using FlowJo (v7.6.1) software, and subtracting the cell size of resting T cells.

Cytotoxicity assays

^{51}Cr-labeled target cell lines were incubated at various rituximab (or ofatumumab, as indicated) concentrations (ranging from 0 to 200 μg/mL) for 30 minutes (at double the final concentration during the initial incubation to yield final concentrations of 10, 25, 50, 100, and 200 μg/mL) before the addition of CAR^+CD8^+ T cells at various effector-to-target (E:T) ratios. Cells were cultured in duplicate at 37°C for 5 hours in medium containing heat-inactivated FBS, with ^{51}Cr-labeled rituximab-blocked target cells in U-bottom 96-well plates. Control wells contained target cells incubated in rituximab-containing medium without T cells (denoted in figures as "0:1" E:T ratio) to exclude the possibility of rituximab/ofatumumab-induced complement-dependent cytotoxicity. Maximal ^{51}Cr release was determined by directly measuring the ^{51}Cr content of supernatants of labeled cells lysed with 5% IGEPAL CA-630. Supernatants were harvested into 96-well Lumaplates, air-dried overnight, and counts were assayed with a TopCount (PerkinElmer). The percentage of cytotoxicity was calculated by the equation: $[\text{Sample} - \text{Min}_{\text{avg}}]/[\text{Max}_{\text{avg}} - \text{Min}_{\text{avg}}] \times 100$.

In vivo assessment of rituximab blocking on CAR T-cell efficacy

Groups of 8-10 NOD.Cg-Prkdc^{scid}Il2rg^{tm1Wjl}/SzJ (NOD/SCID/$\gamma^{-/-}$ [NSG]) mice 6 to 10 weeks of age (The Jackson Laboratory) were inoculated with 5×10^5 rituximab-resistant Raji-ffLuc lymphoma cells 5 days prior to intraperitoneal (i.p.) administration of 25 μg or 200 μg of rituximab. The following day (6 days after tumor inoculation), 10^7 CAR^+ Tcm-derived cells were injected by tail vein. Mouse serum was obtained by centrifugation of clotted blood specimens from the retro-orbital plexus on days 6 and 13 after tumor inoculation, and serum rituximab levels were measured using an ELISA assay to determine rituximab concentrations as previously described (37, 38). Bioluminescence imaging to determine tumor growth was performed as previously described (26). Binning and exposure were adjusted to achieve maximum sensitivity without leading to image saturation. Survival curves were generated using the Kaplan–Meier method with GraphPad Prism 6 software.

To test for the persistence of adoptively transferred T cells, whole blood collected on day 28 by retro-orbital bleeding was lysed by ACK lysing buffer (Quality Biological). Fc receptors of isolated cells were blocked with intravenous immunoglobulin (IVIG), and cells were stained with mAbs to mCD45 (30-F11; Biolegend), hCD3 (HTT3a; Biolegend), and hCD19 (HIB19; BD Bioscience). Data were collected with a BD Canto 2 and analyzed on FlowJo Software (TreeStar). Mouse studies were approved by the FHCRC Institutional Animal Care and Use Committee.

Patient serum samples

Human serum samples were provided by patients with B-cell lymphoma following IRB approval and informed consent obtained in accordance with the Declaration of Helsinki. Serum samples were collected within 4 months after rituximab-containing salvage chemoimmunotherapy, and serum rituximab concentrations were determined (38).

Results

Rituximab blocks CD20 binding of antibodies used to derive CAR scFvs

We previously reported results testing CD20-directed CARs using scFvs derived from two different murine mAbs, Leu16 (L27) or 1F5 (9, 10, 29, 32), each of which binds to epitopes on the large extracellular loop of the CD20 molecule (39). These CD20 epitopes overlap with the rituximab epitope (39), and thus rituximab would be expected to block the binding of these CARs. Using flow cytometry, we tested the ability of various concentrations of rituximab to block binding of the Leu16 mAb coupled to phycoerythrin (Leu16-PE) to CD20 expressed on Ramos lymphoma cells by pre-incubating these cells with rituximab before incubation with the Leu16-PE. As expected, we found a dose-dependent blockade of CD20, with near-complete blockade with rituximab at 50 μg/mL at 4°C. However, when Leu16-PE was incubated at the physiologically relevant 37°C, it bound CD20 to a small extent even at 200 μg/mL of rituximab (Fig. 1). Similar findings were observed in experiments using the 1F5 mAb on FL-18 cells (data not shown). Thus, rituximab binds to overlapping epitopes with our CD20 CARs and has the potential to interfere with CAR T-cell activity against $CD20^+$ target cells.

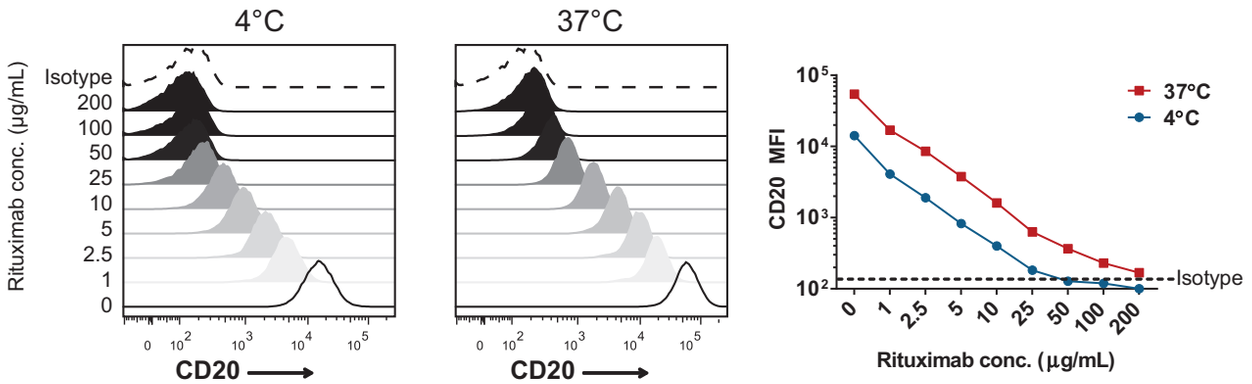

Figure 1.
Rituximab blocks antigen binding of Ab used to derive CAR scFv. Ramos cells (CD20$^+$) were incubated with the indicated rituximab concentrations (conc.) for 30 minutes, followed by incubation with PE-labeled anti-CD20 Ab (clone Leu16) or isotype control at either 4°C or 37°C for 30 minutes. Cells were washed and analyzed by flow cytometry to determine available CD20 binding sites as measured by PE fluorescence intensity. The right panel summarizes the geometric mean fluorescence intensity (MFI) at either 4°C or 37°C as a function of rituximab concentration. The data are representative of three independent experiments.

Impact of rituximab on *in vitro* function of CAR T cells

We assessed the impact of CD20 blocking by rituximab on the function of CD20 CAR T cells by measuring proliferation, cytokine secretion, and cytotoxicity using five different CD20 CAR lentiviral constructs after incubation with a variety of CD20$^+$ B cell NHL cell lines. The CAR constructs (Supplementary Fig. S1A) were the third-generation Leu16-28-BB-z-tEGFR and 1F5-28-BBz constructs (32), the second-generation Leu16-28-z construct, and two CD20 CARs (1.5.3-NQ-28-BB-z and 1.5.3-NQ-28-z) derived from the fully human 1.5.3 mAb to CD20, which also binds to an overlapping epitope with rituximab (36). CAR expression was typically achieved in 40% to 80% of the T cells (Supplementary Fig. S1B).

Proliferation of CFSE-labeled CAR T cells was largely unimpaired when cultured with various NHL target cell lines (Raji, Daudi, Rec-1, and FL-18) in the presence of rituximab. CAR T cells stimulated with target cells in the presence of rituximab at concentrations up to 200 μg/mL exhibited >96% of the proliferation observed after stimulation in the absence of rituximab (Fig. 2A; Supplementary Fig. S2). Cell size is another measure of T-cell activation (40). We analyzed CAR$^+$ T cells by flow cytometry for forward scatter as an estimate of cell size and found that after stimulation with Raji, Daudi, or Rec-1 cells preincubated with rituximab, CAR T cells exhibited a median size >85% of the size of control cells not exposed to rituximab (Fig. 2A). T cells incubated with FL-18 cells exhibited a slightly more pronounced but still modest reduction in cell size after incubation with rituximab (73% of control cell size at 200 μg/mL).

In contrast to proliferation, we found that cytokine secretion by CAR T cells decreased in the presence of increasing rituximab (Fig. 2B). However, even at 100 μg/mL of rituximab, IFNγ, IL2, and TNFα were produced at 34% to 51%, 70% to 92%, and 79% to 108% of baseline, respectively. Similar findings were observed using as target K562 cells genetically modified to express CD80 and CD20, with CD20$^-$ K562-CD80 cells as a control to demonstrate antigen specificity of CD20 CAR T-cell activity (Supplementary Fig. S3).

We also examined the impact of rituximab on the cytolytic activity of CAR$^+$ T cells against various CD20$^+$ NHL target cell lines. Using standard ^{51}Cr-release assays with CAR$^+$CD8$^+$ T cells as effectors and Raji, FL-18, Granta, or Rec-1 as targets, we found that cytotoxicity was minimally impaired in rituximab concentrations of up to 50 μg/mL (Fig. 3), and >65% of baseline cytolytic activity was retained in rituximab concentrations of 100 μg/mL against all target cell lines tested.

We tested the *in vitro* functionality of the fully human 1.5.3-NQ-28-z and 1.5.3-NQ-28-BB-z CAR T cells in the presence of rituximab, and found that, as with the Leu16 and 1F5 CARs, cytokine secretion and cytotoxicity, but not proliferation, decreased modestly in a dose-dependent manner against rituximab-pretreated target cells (Supplementary Fig. S4).

Effect of CD20 antigen expression level

We hypothesized that the amount of CD20 expression on tumor cells might affect sensitivity to rituximab blockade and tested this by selecting K562-CD80 cell lines with low, medium, and high CD20 expression after limiting dilution cloning (Supplementary Fig. S5). We again assessed *in vitro* CAR T-cell function in the presence of varying concentrations of rituximab. As with the NHL cell lines, proliferation of CAR T cells was completely intact regardless of target cell CD20 expression (Fig. 4A). Cell size was undiminished when CD20^{high} cells were used as targets, although a modest reduction in cell size occurred with cells expressing lower levels of CD20. In contrast to proliferation and cell size, cytokine secretion was significantly impaired upon stimulation with CD20^{low} target cells, with IFNγ, IL2, and TNFα levels as low as 5%, 17%, and 22% of baseline values, respectively, at 100–200 μg/mL of rituximab (Fig. 4B; Supplementary Fig. S6), whereas T cells stimulated with CD20^{high} targets retained >75% of baseline activity at rituximab concentrations of 100 μg/mL.

CD20 antigen density affected the rituximab-mediated inhibition of CAR T-cell cytolytic activity (Fig. 4C). T-cell killing of target cells expressing high CD20 was minimally affected by rituximab, even at low E:T ratios. However, T-cell cytotoxicity decreased in a dose-dependent manner against CD20^{low} and CD20^{medium} K562-CD80 targets, which was most pronounced at lower E:T ratios. Cytolytic activity against CD20^{low} targets was retained at 47% of baseline at a 50:1 E:T ratio at 200 μg/mL of rituximab, but was only 16% of baseline at a 2:1 E:T ratio.

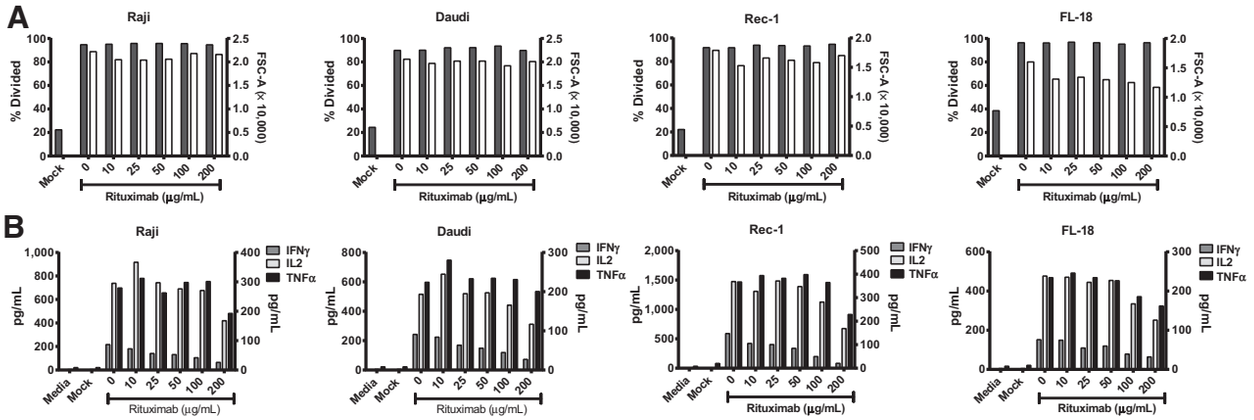

Figure 2.
Effect of rituximab on CAR T-cell function *in vitro*. The indicated B-cell NHL cell lines were irradiated and incubated for 30 minutes at room temperature with varying rituximab concentrations (at two times the concentrations during incubation to yield the indicated final concentrations after addition of T cells). A, CFSE-stained T cells expressing the Leu16-28-BB-z-tEGFR CD20-specific CAR were added to the target cells at a 1:1 volume and ratio. Proliferation of the T cells was analyzed 4 days later by flow cytometry for CFSE dilution. The percentage of divided $CD3^+$ T cells relative to unstimulated T cells is shown on the left axis (filled bars). Histograms of CFSE intensity are shown in Supplementary Fig. S2. Cell size of $CD3^+$ T cells as determined by geometric mean of forward scatter (subtracting size of cells in media only) is shown on the right axis (open bars). B, cytokine secretion of these T cells was measured by the Luminex assay using supernatants from 24 hours after restimulation. IL2 concentrations are shown on the left *y*-axis and IFNγ and TNFα on the right *y*-axis. The data are representative of three independent experiments.

In vivo antitumor activity of CD20 CAR T cells in the presence of residual rituximab

The *in vitro* experiments above suggested that CD20 CAR T cells retain significant functionality against $CD20^+$ tumors despite the presence of moderate levels of rituximab. To evaluate how these observations would translate to the *in vivo* setting, we tested the impact of residual rituximab on CAR T-cell activity in a mouse lymphoma model.

Rituximab as a single agent has significant antitumor activity against Raji cells in immunocompromised mouse xenograft models (41). To overcome a potential confounding therapeutic effect from rituximab in these combination therapy experiments, we generated a rituximab-refractory Raji cell line (RR-Raji) using previously described methods (27), and found that CD20 expression was retained in this cell line (Supplementary Fig. S7).

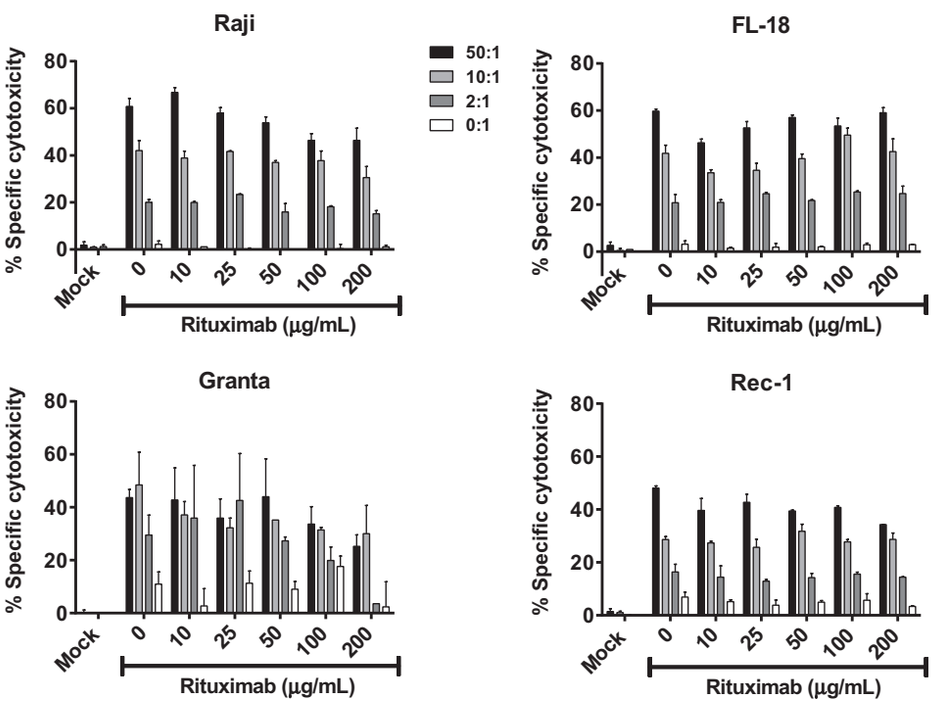

Figure 3.
Effect of rituximab on CAR T-cell–mediated cytotoxicity. The indicated ^{51}Cr-labeled target cells were preincubated for 30 minutes with rituximab (at two times the concentrations during incubation to yield the indicated final concentrations after the addition of T cells), and then $CD8^+$ T cells expressing the Leu16-28-z CAR were added at the E:T ratios shown in a standard 5-hour ^{51}Cr-release assay. Mock-transduced T cells and samples with rituximab and target cells only ("0:1") were used as negative controls. The average value of duplicate wells is shown, with error bars representing standard deviation. The data are representative of results from four independent experiments.

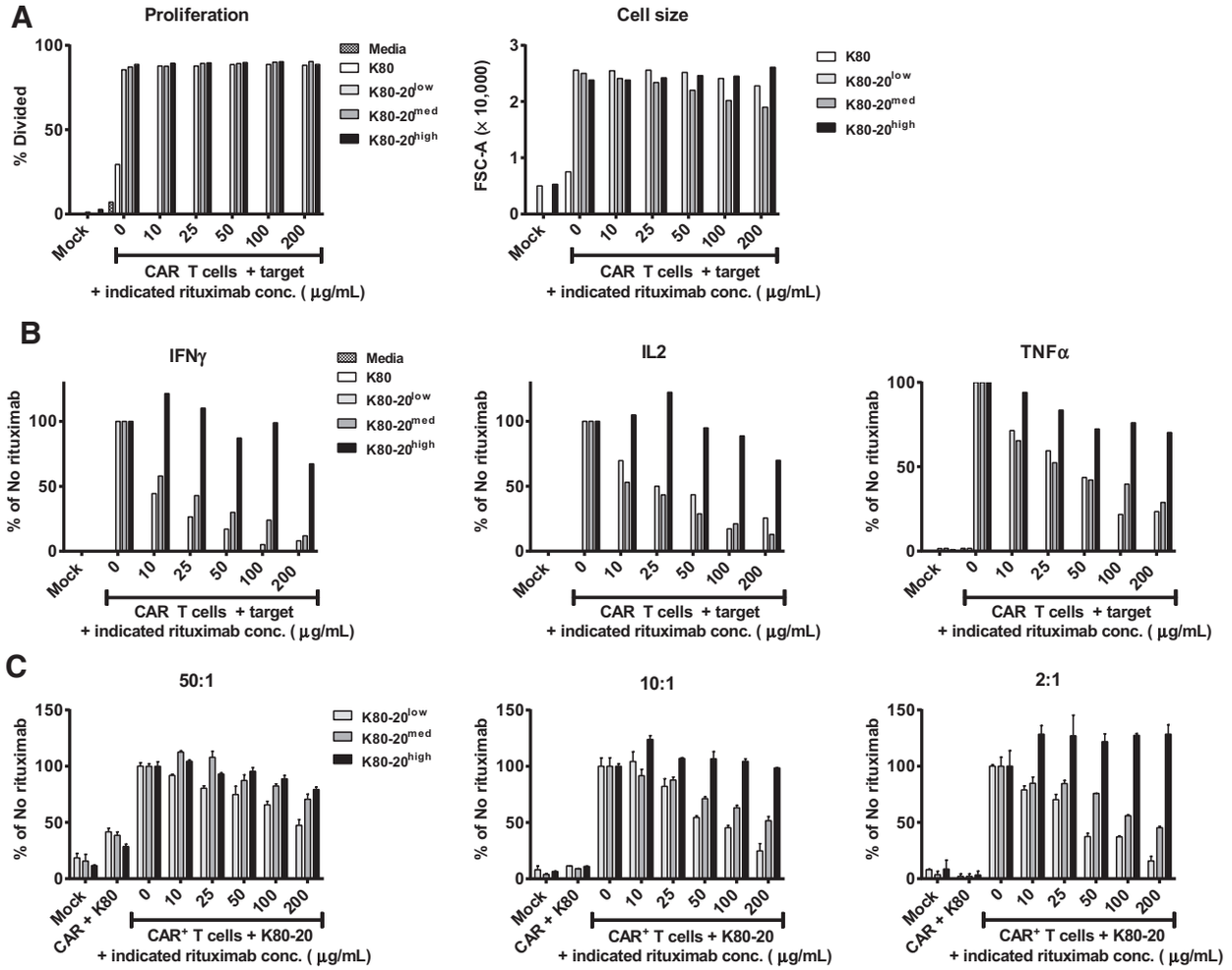

Figure 4.

Sensitivity to rituximab blockade is dependent on CD20 antigen density on target cells. K562 cells transduced with CD80 and CD20 ("K80-20") were cloned by limiting dilution; selected for high, medium, or low levels of CD20 expression (Supplementary Fig. S5); and used as target cells in assays for A, proliferation and cell size (geometric mean forward scatter of gated $CD3^+$ cells minus the size of cells in media only) using CFSE-labeled Leu16-28-z CAR-transduced T cells as described in Fig. 2; B, cytokine secretion of the Leu16-28-z CAR-transduced T cells at 24 hours from A above, measured by Luminex assay; C, cytotoxicity using Leu16-28-z CAR-transduced $CD8^+$ T cells by ^{51}Cr-release assay as described in Fig. 3. Data are representative of three independent experiments. Absolute values for cytokine secretion are shown in Supplementary Fig. S6.

We inoculated NSG mice i.v. with RR-Raji cells and treated some groups with high- or low-dose rituximab 5 days after inoculation, once tumors were established. CD20 CAR^+ T cells were administered i.v. the next day (Fig. 5A). Mice that received rituximab alone showed a modest, transient antitumor effect, but all died of tumor progression by day 24, whereas mice treated with CAR T cells alone had significant tumor regression, with tumor eradication in 40% of mice and a doubling of median survival (52 days). Mice that received rituximab the day before T-cell infusion did not have impaired *in vivo* CAR T-cell activity compared with mice receiving CAR T cells alone; tumors were eradicated in all mice in the group receiving rituximab, 200 μg/mL, and in all but one mouse in the 25-μg/mL group (Fig. 5B and C; Supplementary Fig. S8).

To confirm that these tumor remissions occurred in the presence of physiologically relevant serum concentrations of rituximab, we collected serum from rituximab-treated mice on the day of T-cell infusion and 1 week later and measured serum rituximab. Mice receiving rituximab at 200 μg/mL had an initial median serum rituximab concentration of 138.5 μg/mL (range, 54.5–173.6) and 39.7 μg/mL (range, 1.6–51.9) a week later, and mice receiving 25 μg/mL had a median concentration of 11.7 μg/mL (range, 2.8–17.8) at baseline and 0 μg/mL 1 week after T-cell infusions (Fig. 5D).

We quantified relative circulating CAR T-cell numbers by flow cytometry 28 days after tumor injection. Mice receiving CAR T cells alone or rituximab plus CAR T cells had similar numbers, suggesting that the presence of rituximab did not impair *in vivo* persistence of CAR T cells (Supplementary Fig. S9).

Serum rituximab concentrations of patients treated with salvage rituximab-containing regimens

Because the ultimate goal of these experiments is to inform future CD20 CAR clinical trials, we defined a clinically relevant

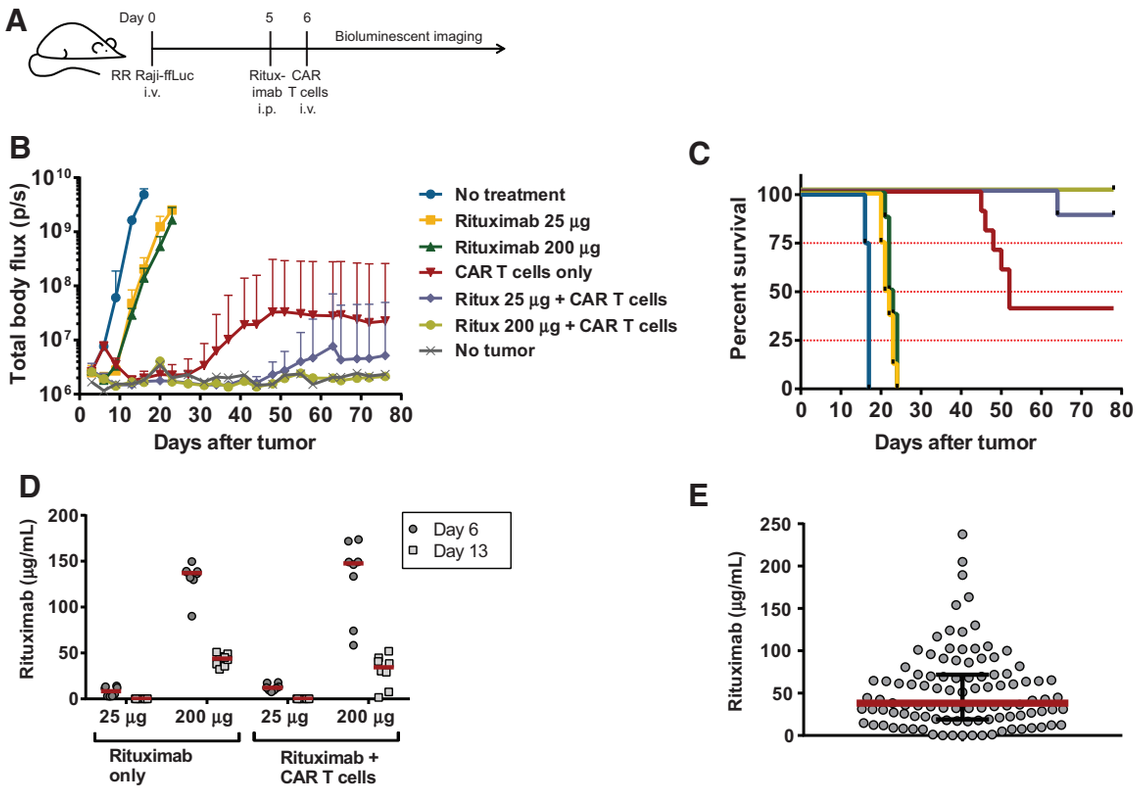

Figure 5.
In vivo effect of rituximab on CD20 CAR T-cell function. NSG mice were injected i.v. with 5×10^5 rituximab-refractory Raji-ffLuc lymphoma cells, followed by one of the following treatments: no treatment, rituximab only (25 μg or 200 μg) i.p. 5 days later, 10^7 1.5.3-NQ-28-BBz CAR T cells only 6 days after tumor, or rituximab 25 μg or 200 μg i.p. at 5 days followed by 10^7 CAR T cells at 6 days after tumor. Mice were imaged twice weekly for bioluminescence. A, schema of mouse experiment. B, average tumor burden per group over time as measured by total body bioluminescence. The geometric mean luminescence values with 95% confidence intervals are shown, and to prevent misleading fluctuations in tumor volume graphs, the last bioluminescence level of each mouse was carried forward after it was killed until no mice in that group remained. Individual bioluminescence traces are shown in Supplementary Fig. S8. C, Kaplan–Meier plot showing overall survival of each treatment group. D, serum rituximab levels on the day of T-cell infusion (day 6) and 1 week after T-cell infusion (day 13). The red lines denote the median values for each group of mice. E, serum rituximab concentrations from lymphoma patients who underwent rituximab-containing salvage chemotherapy within the 4 preceding months. The red line indicates the median, and black lines indicate the interquartile range (25%–75%).

range of residual serum rituximab concentrations in the intended patient population by querying a database of patients with B-cell NHL who underwent autologous stem cell transplantation on investigational protocols at our center and had a pretransplant serum rituximab measurement available (37). We identified 103 patients who received a rituximab-containing chemotherapy regimen within 4 months of the serum blood draw (range, 0.5–3.8 months, median 1.8), and the median rituximab concentration in these patients was 38.3 μg/mL, with an interquartile range of 19.1 to 71.7 μg/mL (Fig. 5E). The rituximab concentration was 100 μg/mL or lower in 86% of patients.

Effect of ofatumumab on CD20 CAR T-cell function

To determine the importance of epitope location on the effect of CD20 mAbs on CAR function, we repeated the *in vitro* assays with ofatumumab, a fully human mAb to CD20 that binds to a distinct epitope involving the smaller extracellular loop of CD20 as well as a different area of the large loop (42, 43).We first evaluated the ability of ofatumumab to block binding of the Leu16 mAb by flow cytometry and found that despite the different epitope, binding of the second antibody was profoundly blocked by ofatumumab, at even lower concentrations than rituximab (Supplementary Fig. S10). We then performed *in vitro* functional assays on Rec-1 and Raji-ffLuc lymphoma cells that had been preincubated with varying concentrations of ofatumumab (Fig. 6). The results were similar to those with rituximab, in that proliferation and cell size were minimally affected, but cytokine production was more affected, in a dose-dependent manner. Compared with rituximab, cytotoxicity was more profoundly impaired in the presence of ofatumumab. These findings suggested that the inhibitory effect of CD20 mAb is due not to direct blocking of the CAR binding epitope, but rather from steric inhibition, and that the stronger inhibitory effect of ofatumumab resulted from a slower off-rate compared with rituximab. This result was supported by competitive cell-binding flow cytometry studies at 4°C or 37°C (Supplementary Fig. S10) that confirmed a much lower dissociation of ofatumumab, consistent with previously reported data (44).

Discussion

In this study we addressed the theoretical concern that CD20-targeted CAR T cells may be rendered ineffective by residual levels of rituximab. This question is relevant to future clinical trials

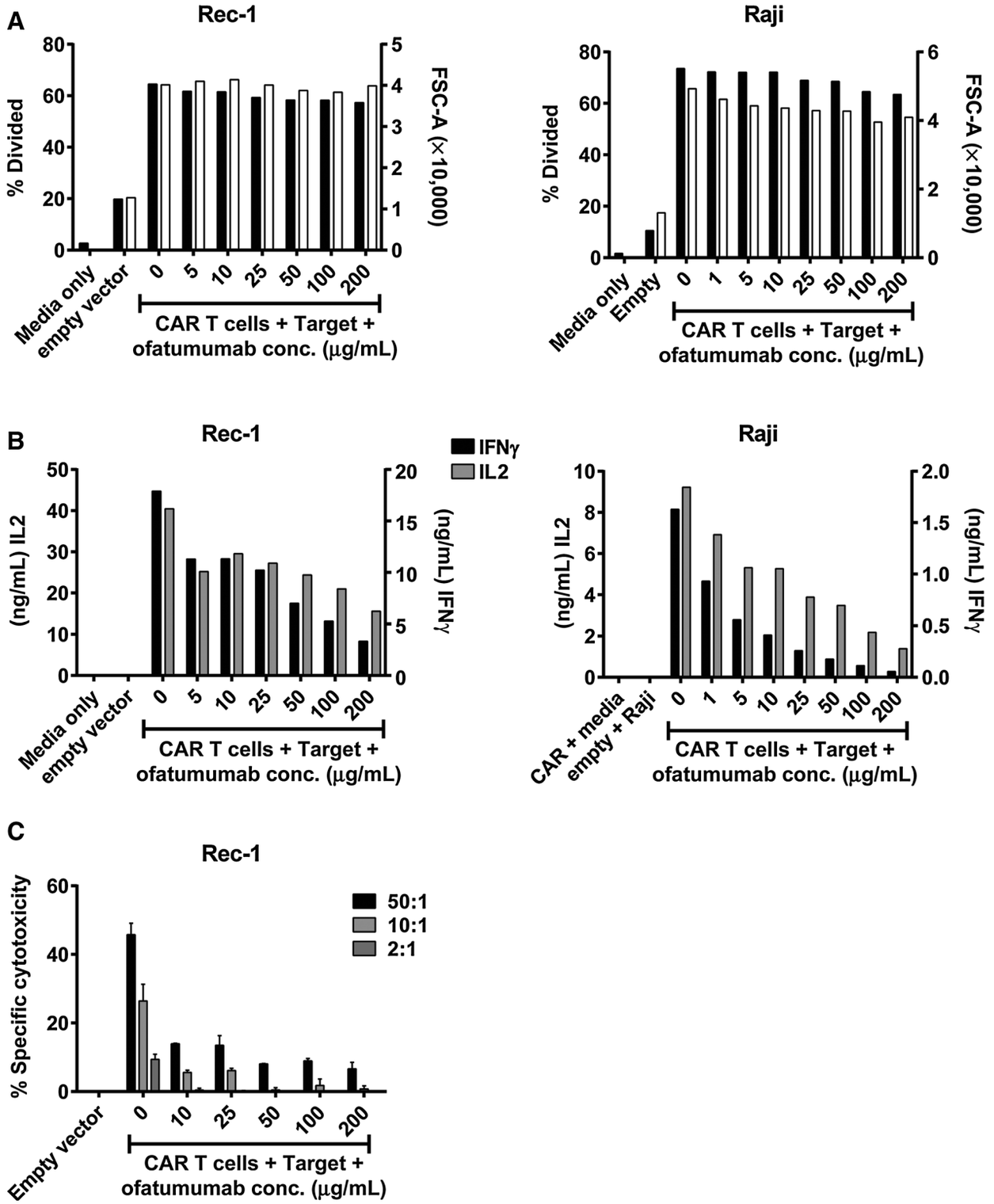

Figure 6.

Effect of ofatumumab on CD20 CAR T-cell function *in vitro*. Irradiated Rec-1 or Raji-ffLuc cells (A and B) or nonirradiated ^{51}Cr-labeled Rec-1 cells (C) were preincubated for 30 minutes with two times the indicated concentrations of ofatumumab, followed by experiments to determine function of T cells expressing the 1.5.3-NQ-28-BB-z CAR, using the methods described in the legends of Figs. 2 and 3. A, the percentage of divided CD3$^+$ T cells relative to unstimulated T cells is shown on the left axis (filled bars). Cell size of CD3$^+$ T cells as determined by geometric mean of forward scatter (subtracting size of cells in media only) is shown on the right axis (open bars). B, cytokine secretion of these T cells was measured by the Luminex assay using supernatants from 24 hours after restimulation. IL2 concentrations are shown on the left *y*-axis and IFNγ on the right *y*-axis. C, cytotoxicity of 1.5.3-NQ-28-BB-z CAR T cells was determined using a standard 4-hour ^{51}Cr-release assay with Rec-1 target cells. The average value of duplicate wells is shown, with error bars representing standard deviation. The data shown each represent a single experiment, with assessment of Rec-1 and Raji targets in independent experiments.

enrolling patients with relapsed or refractory B-cell lymphomas treated recently with rituximab-containing salvage chemotherapy, who may have significant residual serum rituximab concentrations at the time of CAR T-cell infusion.

We defined the range of serum levels of rituximab that would likely be encountered in a CAR T-cell trial by examining a large cohort of patients treated at our center who had received rituximab-containing therapy within the previous 4 months. We found that the vast majority of patients had rituximab of 100 μg/mL or less, with a median value of less than 40 μg/mL. Within this range of rituximab concentrations, CD20-specific CAR T cells maintained significant activity both *in vitro* and *in vivo* despite partial blockade of CAR-binding sites, presumably due to a significant dissociation (off-rate) of rituximab at 37°C that permits CAR triggering to occur. Cytokine secretion and cytotoxicity were impaired *in vitro* in a dose-dependent manner; however, even at rituximab concentrations of 100 μg/mL, CAR T cells generally retained at least half, and usually 60% to 70% or more of their baseline activity, while proliferation was not affected at up to 200 μg/mL of rituximab. Most importantly, CAR T-cell function was not affected *in vivo* in a mouse model in the presence of rituximab concentrations that were significantly higher than the anticipated values of most human patients in future CAR T-cell trials.

The results of the mouse experiment demonstrating superior outcomes in the groups receiving combination therapy compared with mice treated with CAR T cells alone are most likely explained by the transient therapeutic response to rituximab that occurred, despite the relative rituximab resistance of the Raji cell line. This resulted in a smaller tumor burden at the time of CAR T-cell infusion and likely conferred an advantage over mice receiving CAR T cells alone. However, the possibility that a synergistic response occurred in the mice that received both rituximab and CAR T cells cannot be excluded. Regardless, the central observation is that CAR T cells remained active and were not impaired by the presence of rituximab. Furthermore, these experiments also illustrate the clinically relevant point that CAR T cells are potentially effective in treating rituximab-resistant tumors, as long as the mechanism of escape from antibody-based therapy is not antigen loss.

The experiments with ofatumumab provide insight into the mechanism of interference of CD20 mAb on CAR T-cell function. Ofatumumab inhibited CAR T-cell function despite the fact that it binds to a nonoverlapping epitope on CD20 compared with our CARs, suggesting that the primary inhibitory mechanism is steric interference between CD20 and the CAR (or T cell), rather than direct competitive blockade of the binding epitope. The functions most affected by the presence of ofatumumab were, in descending order, cytotoxicity (4-hour assay), cytokine secretion (24-hour assay), and proliferation (96-hour assay). These results highlight the importance of off-rate: the slower dissociation of ofatumumab compared with rituximab manifested as profound impairment of CAR T-cell function over a short time period, but CAR T cells in continuous close contact with target cells over a day or more could become activated.

Our results also provide insights into CAR T-cell biology, with respect to the effect of high or low target antigen expression on CAR T-cell activation, because varying degrees of blockade of CD20 binding sites at different rituximab concentrations may be thought of as a surrogate for antigen density. The observation that CAR T cells effectively kill target cells in the presence of high concentrations of rituximab, even on target cells with low CD20 expression, suggests that very little antigen is required for CAR T-cell lytic activity, consistent with recently reported data (45). In fact, high antigen density may be suboptimal for CAR T-cell activation, at least with respect to cytokine secretion, because low-to-intermediate concentrations of rituximab on target cells with high antigen expression actually increased cytokine production. This concept that an optimal CAR-to-antigen density ratio exists is consistent with previous reports (46).

The results presented here provide reassurance that adoptively transferred CD20-specific CAR T cells are likely to retain major activity even in patients recently treated with rituximab, but a further consideration is that even at high mAb concentrations sufficient to block CAR T-cell activity *in vitro*, complete saturation of intratumoral CD20 sites may not occur. In a clinical trial, 4 patients with refractory malignant B-cell lymphomas treated with continuous i.v. infusions of the murine 1F5 mAb to CD20 had minimal 1F5 binding to malignant lymph node sites at low-to-intermediate serum concentrations (28). Only at high concentrations (>150 μg/mL) was significant Ab binding observed, suggesting poor penetration of the mAb into tumors. It is possible that T cells, by virtue of their ability to extravasate and migrate actively through lymphoid tissue, could access tumor cells in areas not penetrated by Ab, thus further circumventing the potential negative impact of competitively binding Ab therapy.

Although these experiments were limited to the evaluation of the CD20 antigen, our results have potential implications for patients receiving CAR T-cell therapy targeted against any antigen previously targeted with a therapeutic Ab. We provide proof of principle that Ab therapy targeting the same epitope as a CAR does not necessarily preclude use of CAR T cells afterward. This concept is likely to become increasingly relevant as more mAb and mAb–drug conjugates are used to treat a variety of malignancies for which CAR T cells may also be used.

In current clinical practice, rituximab is the most relevant mAb for CD20 CAR T cells, but other CD20 mAbs are becoming more routinely used. The experiments reported here may need to be repeated in the future using these alternative mAbs, particularly those with slower off-rates than rituximab, because our experiments with ofatumumab suggest that such agents may have a more inhibitory effect than rituximab on CD20 CAR T-cell function.

In summary, our results suggest that residual rituximab, within the range of concentrations likely to be encountered in patients with B-cell lymphoma entering CAR T-cell clinical trials, leads to a modest reduction of CAR T-cell function *in vitro*, but *in vivo* antitumor activity remains intact. Thus, prior therapy with rituximab is unlikely to be a major barrier to treatment with CD20 CAR T cells in most patients with lymphoma.

Disclosure of Potential Conflicts of Interest

O.W. Press reports receiving commercial research support from Roche/Genentech and is a consultant/advisory board member for Roche. M.C. Jensen reports receiving commercial research support from, has ownership interest (including patents) in, and is a consultant/advisory board member for Juno Therapeutics, Inc. S.R. Riddell reports receiving commercial research support from Juno Therapeutics, has ownership interest (including patents) in Juno Therapeutics, and is a consultant/advisory board member for Juno Therapeutics and Cell Medica. B.G. Till reports receiving commercial research support from Roche-Genentech. No potential conflicts of interest were disclosed by the other authors.

Authors' Contributions

Conception and design: O.W. Press, A.K. Gopal, L.E. Budde, B.G. Till
Development of methodology: O.W. Press, S.Y. Lee, M.C. Jensen, B. Pender, D.G. Maloney, S.R. Riddell, B.G. Till

Acquisition of data (provided animals, acquired and managed patients, provided facilities, etc.): G.A. Rufener, O.W. Press, P. Olsen, A.K. Gopal, B. Pender, J.K. Rossow, D.G. Maloney, B.G. Till
Analysis and interpretation of data (e.g., statistical analysis, biostatistics, computational analysis): O.W. Press, P. Olsen, S.Y. Lee, A.K. Gopal, B. Pender, D.J. Green, B.G. Till
Writing, review, and/or revision of the manuscript: G.A. Rufener, O.W. Press, A.K. Gopal, L.E. Budde, D.J. Green, D.G. Maloney, S.R. Riddell, B.G. Till
Administrative, technical, or material support (i.e., reporting or organizing data, constructing databases): G.A. Rufener, P. Olsen, B. Pender, B.G. Till
Study supervision: G.A. Rufener, B.G. Till

Grant Support

B.G. Till is a Damon Runyon-Pfizer Clinical Investigator (grant 49-C10). This work was also supported by the Giuliani Family Foundation (PI: O.W. Press), NIH/NCI K23CA154874 (PI: B.G. Till), NIH/NCI Cancer Center Support Grant P30CA015704 both for Shared Resources (P.I.: Gary Gilliland) and also as a Recruitment Award (Sub-project PI: B.G. Till), NIDDK DK56465 (PI: Shelly Heimfeld, core resources), NIH/NCI P01CA044991, NIH/NCI K24CA184039 (PI: A.K. Gopal), NIH/NCI K08CA151682 (PI: D.J. Green), and Lymphoma Research Foundation MCL-1003440 (PI: A.K. Gopal).

The costs of publication of this article were defrayed in part by the payment of page charges. This article must therefore be hereby marked *advertisement* in accordance with 18 U.S.C. Section 1734 solely to indicate this fact.

Received November 17, 2015; revised February 22, 2016; accepted March 9, 2016; published OnlineFirst April 21, 2016.

References

1. Brentjens RJ, Davila ML, Riviere I, Park J, Wang X, Cowell LG, et al. CD19-Targeted T cells rapidly induce molecular remissions in adults with chemotherapy-refractory acute lymphoblastic leukemia. Sci Transl Med 2013;5:177ra38.
2. Haso W, Lee DW, Shah NN, Stetler-Stevenson M, Yuan CM, Pastan IH, et al. Anti-CD22-chimeric antigen receptors targeting B-cell precursor acute lymphoblastic leukemia. Blood 2013;121:1165–74.
3. James SE, Greenberg PD, Jensen MC, Lin Y, Wang J, Till BG, et al. Antigen sensitivity of CD22-specific chimeric TCR is modulated by target epitope distance from the cell membrane. J Immunol 2008;180:7028–38.
4. Kalos M, Levine BL, Porter DL, Katz S, Grupp SA, Bagg A, et al. T cells with chimeric antigen receptors have potent antitumor effects and can establish memory in patients with advanced leukemia. Sci Transl Med 2011;3:95ra73.
5. Kochenderfer JN, Dudley ME, Kassim SH, Somerville RP, Carpenter RO, Stetler-Stevenson M, et al. Chemotherapy-refractory diffuse large B-cell lymphoma and indolent B-cell malignancies can be effectively treated with autologous T cells expressing an anti-CD19 chimeric antigen receptor. J Clin Oncol 2015;33:540–9.
6. Lee DW, Kochenderfer JN, Stetler-Stevenson M, Cui YK, Delbrook C, Feldman SA, et al. T cells expressing CD19 chimeric antigen receptors for acute lymphoblastic leukaemia in children and young adults: a phase 1 dose-escalation trial. Lancet 2015;385:517–28.
7. Porter DL, Hwang WT, Frey NV, Lacey SF, Shaw PA, Loren AW, et al. Chimeric antigen receptor T cells persist and induce sustained remissions in relapsed refractory chronic lymphocytic leukemia. Sci Transl Med 2015;7:303ra139.
8. Savoldo B, Ramos CA, Liu E, Mims MP, Keating MJ, Carrum G, et al. CD28 costimulation improves expansion and persistence of chimeric antigen receptor-modified T cells in lymphoma patients. J Clin Invest 2011;121:1822–6.
9. Till BG, Jensen MC, Wang J, Chen EY, Wood BL, Greisman HA, et al. Adoptive immunotherapy for indolent non-Hodgkin lymphoma and mantle cell lymphoma using genetically modified autologous CD20-specific T cells. Blood 2008;112:2261–71.
10. Till BG, Jensen MC, Wang J, Qian X, Gopal AK, Maloney DG, et al. CD20-specific adoptive immunotherapy for lymphoma using a chimeric antigen receptor with both CD28 and 4-1BB domains: pilot clinical trial results. Blood 2012;119:3940–50.
11. Coiffier B, Lepage E, Briere J, Herbrecht R, Tilly H, Bouabdallah R, et al. CHOP chemotherapy plus rituximab compared with CHOP alone in elderly patients with diffuse large-B-cell lymphoma. N Engl J Med 2002;346:235–42.
12. Lenz G, Dreyling M, Hoster E, Wormann B, Duhrsen U, Metzner B, et al. Immunochemotherapy with rituximab and cyclophosphamide, doxorubicin, vincristine, and prednisone significantly improves response and time to treatment failure, but not long-term outcome in patients with previously untreated mantle cell lymphoma: results of a prospective randomized trial of the German Low Grade Lymphoma Study Group (GLSG). J Clin Oncol 2005;23:1984–92.
13. Marcus R, Imrie K, Solal-Celigny P, Catalano JV, Dmoszynska A, Raposo JC, et al. Phase III study of R-CVP compared with cyclophosphamide, vincristine, and prednisone alone in patients with previously untreated advanced follicular lymphoma. J Clin Oncol 2008;26:4579–86.
14. Pfreundschuh M, Kuhnt E, Trumper L, Osterborg A, Trneny M, Shepherd L, et al. CHOP-like chemotherapy with or without rituximab in young patients with good-prognosis diffuse large-B-cell lymphoma: 6-year results of an open-label randomised study of the MabThera International Trial (MInT) Group. Lancet Oncol 2011;12:1013–22.
15. Pulczynski S, Boesen AM, Jensen OM. Antibody-induced modulation and intracellular transport of CD10 and CD19 antigens in human B-cell lines: an immunofluorescence and immunoelectron microscopy study. Blood 1993;81:1549–57.
16. Press OW, Howell-Clark J, Anderson S, Bernstein I. Retention of B-cell-specific monoclonal antibodies by human lymphoma cells. Blood 1994;83:1390–7.
17. Pulczynski S, Boesen AM, Jensen OM. Modulation and intracellular transport of CD20 and CD21 antigens induced by B1 and B2 monoclonal antibodies in RAJI and JOK-1 cells–an immunofluorescence and immunoelectron microscopy study. Leuk Res 1994;18:541–52.
18. Grupp SA, Kalos M, Barrett D, Aplenc R, Porter DL, Rheingold SR, et al. Chimeric antigen receptor-modified T cells for acute lymphoid leukemia. N Engl J Med 2013;368:1509–18.
19. Gall JM, Davol PA, Grabert RC, Deaver M, Lum LG. T cells armed with anti-CD3 x anti-CD20 bispecific antibody enhance killing of CD20+ malignant B cells and bypass complement-mediated rituximab resistance in vitro. Exp Hematol 2005;33:452–9.
20. Jensen M, Tan G, Forman S, Wu AM, Raubitschek A. CD20 is a molecular target for scFvFc:zeta receptor redirected T cells: implications for cellular immunotherapy of CD20+ malignancy. Biol Blood Marrow Transplant 1998;4:75–83.
21. Jensen MC, Cooper LJ, Wu AM, Forman SJ, Raubitschek A. Engineered CD20-specific primary human cytotoxic T lymphocytes for targeting B-cell malignancy. Cytotherapy 2003;5:131–8.
22. Hombach A, Heuser C, Gerken M, Fischer B, Lewalter K, Diehl V, et al. T cell activation by recombinant FcepsilonRI gamma-chain immune receptors: an extracellular spacer domain impairs antigen-dependent T cell activation but not antigen recognition. Gene Ther 2000;7:1067–75.
23. Hombach A, Koch D, Sircar R, Heuser C, Diehl V, Kruis W, et al. A chimeric receptor that selectively targets membrane-bound carcinoembryonic antigen (mCEA) in the presence of soluble CEA. Gene Ther 1999;6:300–4.
24. Nolan KF, Yun CO, Akamatsu Y, Murphy JC, Leung SO, Beecham EJ, et al. Bypassing immunization: optimized design of "designer T cells" against carcinoembryonic antigen (CEA)-expressing tumors, and lack of suppression by soluble CEA. Clin Cancer Res 1999;5:3928–41.
25. Westwood JA, Murray WK, Trivett M, Haynes NM, Solomon B, Mileshkin L, et al. The Lewis-Y carbohydrate antigen is expressed by many human tumors and can serve as a target for genetically redirected T cells despite the presence of soluble antigen in serum. J Immunother 2009;32:292–301.
26. James SE, Orgun NN, Tedder TF, Shlomchik MJ, Jensen MC, Lin Y, et al. Antibody-mediated B-cell depletion before adoptive immunotherapy with T cells expressing CD20-specific chimeric T-cell receptors facilitates

eradication of leukemia in immunocompetent mice. Blood 2009;114: 5454–63.
27. Czuczman MS, Olejniczak S, Gowda A, Kotowski A, Binder A, Kaur H, et al. Acquirement of rituximab resistance in lymphoma cell lines is associated with both global CD20 gene and protein down-regulation regulated at the pretranscriptional and posttranscriptional levels. Clin Cancer Res 2008;14:1561–70.
28. Press OW, Appelbaum F, Ledbetter JA, Martin PJ, Zarling J, Kidd P, et al. Monoclonal antibody 1F5 (anti-CD20) serotherapy of human B cell lymphomas. Blood 1987;69:584–91.
29. Wang J, Jensen M, Lin Y, Sui X, Chen E, Lindgren CG, et al. Optimizing adoptive polyclonal T cell immunotherapy of lymphomas, using a chimeric T cell receptor possessing CD28 and CD137 costimulatory domains. Hum Gene Ther 2007;18:712–25.
30. Wang J, Press OW, Lindgren CG, Greenberg P, Riddell S, Qian X, et al. Cellular immunotherapy for follicular lymphoma using genetically modified CD20-specific CD8+ cytotoxic T lymphocytes. Mol Ther 2004;9: 577–86.
31. Hudecek M, Lupo-Stanghellini MT, Kosasih PL, Sommermeyer D, Jensen MC, Rader C, et al. Receptor affinity and extracellular domain modifications affect tumor recognition by ROR1-specific chimeric antigen receptor T cells. Clin Cancer Res 2013;19:3153–64.
32. Budde LE, Berger C, Lin Y, Wang J, Lin X, Frayo SE, et al. Combining a CD20 chimeric antigen receptor and an inducible caspase 9 suicide switch to improve the efficacy and safety of T cell adoptive immunotherapy for lymphoma. PLoS One 2013;8:e82742.
33. Becker PS, Taylor JA, Trobridge GD, Zhao X, Beard BC, Chien S, et al. Preclinical correction of human Fanconi anemia complementation group A bone marrow cells using a safety-modified lentiviral vector. Gene Ther 2010;17:1244–52.
34. Hudecek M, Sommermeyer D, Kosasih PL, Silva-Benedict A, Liu L, Rader C, et al. The nonsignaling extracellular spacer domain of chimeric antigen receptors is decisive for in vivo antitumor activity. Cancer Immunol Res 2015;3:125–35.
35. Hombach A, Hombach AA, Abken H. Adoptive immunotherapy with genetically engineered T cells: modification of the IgG1 Fc `spacer' domain in the extracellular moiety of chimeric antigen receptors avoids `off-target' activation and unintended initiation of an innate immune response. Gene Ther 2010;17:1206–13.
36. Bornstein GG, Queva C, Tabrizi M, van Abbema A, Chavez C, Wang P, et al. Development of a new fully human anti-CD20 monoclonal antibody for the treatment of B-cell malignancies. Invest New Drugs 2010;28:561–74.
37. Gopal AK, Press OW, Wilbur SM, Maloney DG, Pagel JM. Rituximab blocks binding of radiolabeled anti-CD20 antibodies (Ab) but not radiolabeled anti-CD45 Ab. Blood 2008;112:830–5.
38. Maloney DG, Grillo-Lopez AJ, White CA, Bodkin D, Schilder RJ, Neidhart JA, et al. IDEC-C2B8 (Rituximab) anti-CD20 monoclonal antibody therapy in patients with relapsed low-grade non-Hodgkin's lymphoma. Blood 1997;90:2188–95.
39. Polyak MJ, Deans JP. Alanine-170 and proline-172 are critical determinants for extracellular CD20 epitopes; heterogeneity in the fine specificity of CD20 monoclonal antibodies is defined by additional requirements imposed by both amino acid sequence and quaternary structure. Blood 2002;99:3256–62.
40. Grumont R, Lock P, Mollinari M, Shannon FM, Moore A, Gerondakis S. The mitogen-induced increase in T cell size involves PKC and NFAT activation of Rel/NF-kappaB-dependent c-myc expression. Immunity 2004;21:19–30.
41. Hernandez-Ilizaliturri FJ, Jupudy V, Ostberg J, Oflazoglu E, Huberman A, Repasky E, et al. Neutrophils contribute to the biological antitumor activity of rituximab in a non-Hodgkin's lymphoma severe combined immunodeficiency mouse model. Clin Cancer Res 2003;9:5866–73.
42. Du J, Yang H, Guo Y, Ding J. Structure of the Fab fragment of therapeutic antibody ofatumumab provides insights into the recognition mechanism with CD20. Mol Immunol 2009;46:2419–23.
43. Teeling JL, Mackus WJ, Wiegman LJ, van den Brakel JH, Beers SA, French RR, et al. The biological activity of human CD20 monoclonal antibodies is linked to unique epitopes on CD20. J Immunol 2006;177:362–71.
44. Teeling JL, French RR, Cragg MS, van den Brakel J, Pluyter M, Huang H, et al. Characterization of new human CD20 monoclonal antibodies with potent cytolytic activity against non-Hodgkin lymphomas. Blood 2004;104: 1793–800.
45. Watanabe K, Terakura S, Martens AC, van Meerten T, Uchiyama S, Imai M, et al. Target antigen density governs the efficacy of anti-CD20-CD28-CD3 zeta chimeric antigen receptor-modified effector $CD8^+$ T cells. J Immunol 2014;194:911–20.
46. Alvarez-Vallina L, Russell SJ. Efficient discrimination between different densities of target antigen by tetracycline-regulatable T bodies. Hum Gene Ther 1999;10:559–63.